Geol. Mag. **147** (5), 2010, pp. 737–749. © Cambridge University Press 2010
doi:10.1017/S0016756810000063

Pan-African metamorphic and magmatic rocks of the Khanka Massif, NE China: further evidence regarding their affinity

JIAN-BO ZHOU*†, SIMON A. WILDE*‡, GUO-CHUN ZHAO§, XING-ZHOU ZHANG*, CHANG-QING ZHENG*, HU WANG* &WEI-SHUN ZENG*

*College of Earth Sciences, Jilin University, Changchun 130061, China
‡Department of Applied Geology, Curtin University of Technology, GPO Box U1987, Perth, WA 6845, Australia
§Department of Earth Sciences, The University of Hong Kong, Pokfulam Road, Hong Kong, China

(*Received* 25 September 2009; *accepted* 24 December 2009; First published online 10 February 2010)

Abstract – The Khanka Massif is a crustal block located along the eastern margin of the Central Asian Orogenic Belt (CAOB) and bordered to the east by Late Jurassic–Early Cretaceous circum-Pacific accretionary complexes of the Eastern Asian continental margin. It consists of graphite-, sillimanite- and cordierite-bearing gneisses, carbonates and felsic paragneisses, in association with various orthogneisses. Metamorphic zircons from a sillimanite gneiss from the Hutou complex yield a weighted mean $^{206}Pb/^{238}U$ age of 490 ± 4 Ma, whereas detrital zircons from the same sample give ages from 934–610 Ma. Magmatic zircon cores in two garnet-bearing granite gneiss samples, also collected from the Hutou complex, yield weighted mean $^{206}Pb/^{238}U$ ages of 522 ± 5 Ma and 515 ± 8 Ma, whereas their metamorphic rims record $^{206}Pb/^{238}U$ ages of 510–500 Ma. These data indicate that the Hutou complex in the Khanka Massif records early Palaeozoic magmatic and metamorphic events, identical in age to those in the Mashan Complex of the Jiamusi Massif to the west. The older zircon populations in the sillimanite gneiss indicate derivation from Neoproterozoic sources, as do similar rocks in the Jiamusi Massif. These data confirm that the Khanka Massif has a close affinity with other major components of the CAOB to the west of the Dun-Mi Fault. Based on these results and previously published data, the Khanka Massif is therefore confirmed as having formed a single crustal entity with the Jiamusi (and possibly the Bureya) massif since Neoproterozoic time.

Keywords: SHRIMP U–Pb dating, Neoproterozoic, Late Pan-African, granulites, Khanka Massif.

1. Introduction

Northeast China and adjacent regions form part of the central East Asian continent and include both the Central Asian Orogenic Belt (CAOB) and Late Jurassic–Early Cretaceous circum-Pacific accretion complexes developed between the Siberian and North China cratons (Fig. 1a). The Khanka Massif was considered to extend northward into the Jiamusi-Bureya Massif near the border of NE China with the Russian Far East, and has been referred to as the Khanka-Jiamusi-Bureya Massif (Natal'in & Borukayev, 1991; Natal'in, 1991, 1993; Cao *et al*. 1992; Şengör, Natal'in & Burtman, 1993; Şengör & Natal'in, 1996). The Yanji-Heilongjiang Fault (F2 and F3, Fig. 1a) was regarded as the suture zone developed between the Khanka-Jiamusi and Songliao massifs (Fig. 1a). However, Shao & Tang (1995), Shao, Tang & Zhan (1995) and Ren *et al.* (1999) have argued that the Khanka Massif was an exotic block, because it contains mixed Permian faunas which are characterized by both palaeo-tropical Cathaysian taxa and cool-temperate elements (Tang, 1990; Tang *et al.* 1995; Shao & Tang, 1995; Shao, Tang & Zhan, 1995; Ren *et al.* 1999). Furthermore, Zhang (1997, 2004) and Zhang, Cai & Zhu (2006) have proposed a tectonic model whereby the Khanka Massif has an affinity to the South China Craton, and the Yanji zone and Dunhua-Mishan (Dun-Mi) Fault was the Triassic suture zone marking the eastern extension of the Qingling-Dabie-Sulu HP–UHP collisional belt between the North China Craton and South China Craton. They thus renamed it the Qingling-Dabie-Tanlu-Sulu-Imjiangang-Yanji zone (Zhang, 1997, 2004; Zhang, Cai & Zhu, 2006). Oh (2006) and Oh, Kim & Williams (2006) supported the view that the Qingling-Dabie-Sulu HP–UHP belt extends through the Korean peninsula to the Yanji zone in NE China. Ishiwatari & Tsujimori (2001, 2003) further suggested that the Yanji zone should be linked with the Heilongjiang blueschist belt (Yanji-Heilongjiang HP belt; see Fig. 1a) at the western margin of the Jiamusi-Khanka Massif. Such scenarios mean that not only the Khanka, but also the Jiamusi and Bureya massifs would possibly belong to the South China Craton. More recently, however, Wu *et al*. (2007) and Wilde, Wu & Zhao (2010) have argued that the Heilongjiang blueschist belt was a Jurassic metamorphic belt and that the Jiamusi-Bureya-Khanka Massif was not an original part of the CAOB but an exotic massif that was accreted to the CAOB in the Jurassic. More recently, Zhou *et al.* (2009) have reported evidence from the Heilongjiang Complex that mafic ocean crust

†Author for correspondence: zhoujb@jlu.edu.cn

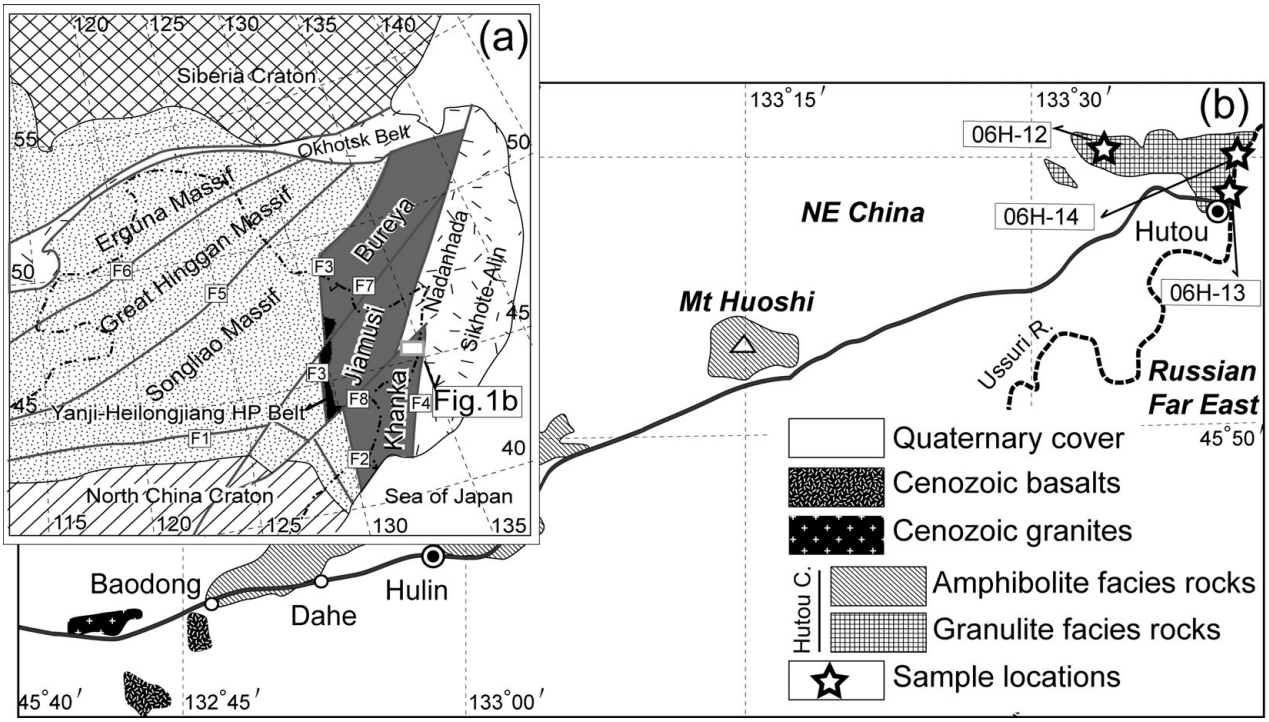

Figure 1. (a) Tectonic sketch map of NE China and Far East Russia (after Wilde, Zhang & Wu, 2000; Wu *et al.* 2007) emphasizing position of the Bureya, Jiamusi and Khanka massifs. Rectangle shows study area. F1 – Inner Mongolia-Jilin Fault; F2 – Yanji Fault; F3 – Mudanjiang Fault; F2+F3 – Yanji-Heilongjiang Fault; F4 – Primoria Fault; F5 – Hegenshan-Heihe Fault; F6 – Xinlin-Xiguitu Fault; F7 – Yilan-Yitong Fault, and F8 – Dunhua-Mishan Fault. (b) Simplified geological sketch map of the northern part of the Chinese segment of the Khanka Massif, showing sample locations.

was generated in the Triassic when the Jiamusi Massif broke away from the Songliao block, only to collide with it again in the latest Triassic to Early Jurassic.

In this paper, we present additional SHRIMP U–Pb zircon data for granulite-facies paragneiss and crustal-derived granites of the Hutou complex in the eastern Khanka Massif along the border between NE China and Far East Russia (Fig. 1a, b). These data not only enable evaluation of protolith ages of the basement rocks, but also allow us to identify the timing of the high-grade metamorphic event. The results provide important insights into the possible link between the Jiamusi and Khanka massifs, and therefore their relationship to the Palaeozoic Central Asian Orogenic Belt.

2. Geological setting

NE China and adjacent regions, including the Russian Far East, have traditionally been considered as the eastern part of the Central Asian Orogenic Belt, located between the Siberian and North China cratons (Natal'in, 1991, 1993; Natal'in & Borukayev, 1991; Şengör & Natal'in, 1996; Şengör, Natal'in & Burtman, 1993; Ren *et al.* 1999; Jahn, Wu & Chen, 2000; Jahn, 2004; Li, 2006). The area consists of a collage of micro-continental blocks (Tang, 1990; Tang *et al.* 1995; Li *et al.* 1999; Li, 2006; Wu *et al.* 2007). In the extreme eastern part of the CAOB, the tectonic units include the Nadanhada Terrane to the northeast, the Songliao Massif in the southwest, the Jiamusi and Khanka massifs in the central area and the North China Craton to the south, separated by the Yanji and Dun-Mi faults (Fig. 1a).

The Nadanhada Terrane is located to the east of the Jiamusi Massif and is part of the Late Jurassic–Early Cretaceous circum-Pacific accretionary belt. It is composed of Jurassic clastic sedimentary rocks, with enclosed tectonic slices of Middle Jurassic siliceous shale, Late Triassic bedded chert and mafic igneous rocks, all intruded by bodies of Cretaceous granites (Kojima, 1989; Cheng *et al.* 2006). Recent zircon U–Pb dating indicates that these granites formed at 131–115 Ma (Cheng *et al.* 2006), whereas a gabbro in the Raohe Complex was emplaced at 166 ± 1 Ma (Cheng *et al.* 2006). Radiolarians in the oceanic sediments have been dated at about 150 Ma (Cheng *et al.* 2006). Therefore, it is concluded that emplacement of igneous plutons in the Nadanhada Terrane took place in the Late Jurassic–Early Cretaceous (Kojima, 1989; Cheng *et al.* 2006), indicating that Pacific plate subduction was active at this time. The lithological association, radiolarian assemblages, ages and geological structure of the Nadanhada Terrane suggest that it consists in part of an ophiolite complex, similar to the Sikhote-Alin complex of the Russian Far East (Kojima, 1989; Zyabrev & Matsuoka, 1999) and the Tamba-Mino-Ashio terrane in Japan (Kojima, 1989).

The Songliao Massif is buried beneath the Songliao sedimentary basin, but petrographic examination of drill core obtained during petroleum exploration reveals that most of the basement rocks are granitic, overlain by Palaeozoic sedimentary strata that have

https://doi.org/10.1017/S0016756810000063 Published online by Cambridge University Press

undergone weak metamorphism and deformation (Wu *et al.* 2000). Wang *et al.* (2007) obtained detrital zircon SHRIMP U–Pb ages ranging from 2.2 to 0.4 Ga from samples of metasedimentary rock. In a drill hole to the southeast of the Songliao Basin, a quartz schist contains zircon populations at *c.* 0.5 Ga, 1.0–1.1 Ga, 1.4–1.5 Ga and 1.7–1.8 Ga (Wang *et al.* 2007), which indicate that the basement of the Songliao Basin is complex and implies that the > 1.4 Ga zircons perhaps originated from the North China Craton, while the 0.5 Ga zircons may have been derived from the Jiamusi Massif (Wang *et al.* 2007). The eastern and northern Songliao Massif is bounded, respectively, by the Zhangguangcai and Lesser Xing'an ranges, which are characterized by voluminous syn-collisional Mesozoic granitic rocks, interpreted to have been generated by westward subduction of the Jiamusi Massif beneath the Songliao Massif during the Mesozoic (215– 185 Ma; Wu *et al.* 2003, 2007).

The Jiamusi Massif contains four main rock associations: the Mashan Complex, which was metamorphosed to granulite facies in the Early Palaeozoic at *c.* 500 Ma (Wilde, Dorsett-Bain & Liu, 1997; Wilde, Zhang & Wu, 2000), deformed Early Palaeozoic granitoids, also metamorphosed to granulite facies by the same event (Li *et al.* 1999; Li, 2006; Wu *et al.* 2001, 2007; Wilde, Wu & Zhang, 2003), undeformed Permian granitoids that intrude the previous rock sequences (Wilde, Dorsett-Bain & Liu, 1997), and the Heilongjiang Complex, an accretionary terrane composed of basalt and clastic and chemical sediments, metamorphosed to epidote-blueschist facies between 210 and 180 Ma (Zhou *et al.* 2009). The Mashan Complex is of particular relevance, since rocks in the Khanka Massif were considered to belong to this series when the latter area was mapped by the Chinese Geological Survey (HBGMR, 1993). It consists of khondalitic rocks with a tight clockwise *P*/*T* path (Jiang, 1992; Lennon, Wilde & Yang, 1997). Peak temperatures were up to 850 °C and pressures attained 0.74 GPa (Jiang, 1992). In the northern part of the Jiamusi Massif (Fig. 1a), the Mashan Complex is at amphibolite facies and characterized by peak temperatures of ∼ 650 °C (garnet-biotite), but locally only reaching 500–550 °C at pressures of 0.6–0.7 GPa (Cao *et al.* 1992). It was originally considered to be Late Archaean in age (HBGMR, 1993), but U–Pb SHRIMP zircon work has shown that the oldest protoliths are Mesoproterozoic and that the complex underwent metamorphism in the Early Palaeozoic at *c.* 500 Ma (Wilde, Dorsett-Bain & Liu, 1997; Wilde, Zhang & Wu, 2000).

The Khanka Massif is located to the south of the Jiamusi Massif (Fig. 1a), with the boundary marked by the Dun-Mi Fault (Jia *et al.* 2004). To the south lies the North China Craton and to the southwest is the Songliao Massif, separated by the Yanji Suture (Jia *et al.* 2004) (Fig. 1a). The Khanka Massif was considered to be composed of Precambrian metamorphosed basement rocks, covered by Palaeozoic to Mesozoic strata, including carbonates, clastic sediments and volcanic rocks (Natal'in, 1993; Shao & Tang, 1995; Shao, Tang & Zhan, 1995; Jia *et al.* 2004; Shi & Zhan, 1996; Shi, 2006). The Chinese portion of the Khanka Massif crops out in only three small areas (Fig. 1b); the most easterly of these is at Hutou. Regional mapping (HBGMR, 1993) has shown a westward decrease in metamorphic grade from granulite to amphibolite facies. The rocks at Hutou form a high-grade metamorphic complex, located around Khanka Lake (Xingka) along the border between NE China and Far East Russia. The granulite-facies rocks mostly consist of graphite-, sillimanite- and cordierite-bearing gneisses, carbonates and felsic paragneisses, together with garnet-bearing granite gneisses. More than 70 % of the outcrop consists of sillimanite- and garnet-bearing granite gneisses that represent crustal melts. The amphibolite-facies rocks predominantly crop out at Mt Huoshi (Fig. 1b) and consist of felsic paragneisses and hornblende schists. Both outcrop areas have been considered to form part of the Mashan 'group' on the regional geological map and were considered to be Late Archaean in age (Zhao, Peng & Dang, 1995; HBGMR, 1993), although no geochronological work was undertaken.

No data are available on the metamorphic conditions of the Khanka Massif at Hutou. However, it consists essentially of a khondalite series in association with sillimanite-garnet granite gneiss, similar to the Mashan Complex of the Jiamusi Massif (HBGMR, 1993; Wilde, Zhang & Wu, 2000). At Hutuo, the garnet-sillimanite paragneiss has a typical mineral assemblage of Grt+Crd+Sill+Bt+Kfs+Pl+Qtz and the sillimanite-garnet granite gneiss has a mineral assemblage of Grt+Sill+Bt+Kfs+Pl+Qtz. As noted above, these rocks are characterized by a tight clockwise *P*/*T* path (Jiang, 1992; Lennon, Wilde & Yang, 1997), with a peak temperature of ∼ 850 °C and pressure of ∼ 0.74 GPa (Jiang, 1992; Wilde, Dorsett-Bain & Liu, 1997).

Recently, Wilde, Wu & Zhao (2010) have presented data for orthogneisses and a fine-grained granitic gneiss from Hutou and Mt Huoshi. However, they did not date either the sillimanite-bearing paragneisses or granite gneiss containing sillimanite. In this study, we have specifically targeted representative samples of these lithologies in order to compare their ages with the orthogneisses and, more importantly, with both the timing of magmatism and high-grade metamorphism in the Jiamusi Massif.

3. Sample locations and descriptions

Samples of paragneiss and garnet-bearing granite gneiss were collected from Hutou at the northern margin of the Chinese segment of the Khanka Massif (Fig. 1b). A single sample of paragneiss and two samples of sillimanite-garnet-bearing granite gneiss were chosen for analysis (Fig. 1b).

https://doi.org/10.1017/S0016756810000063 Published online by Cambridge University Press

3.a. Paragneiss

A sample of sillimanite gneiss (06H-12) was collected 3 km NW of Hutou (Fig. 1b). It is composed of laths of sillimanite (5 %), up to 1 mm long (Fig. 2a, b), showing a strong preferred orientation. The sillimanite is associated with weakly elongated quartz (40 %) with curved to lobate grain boundaries. Other minerals are porphyroblasts of garnet (15 %) (Fig. 2a, b) and cordierite (8 %) (Fig. 2c, d), with some biotite (5 %), alkali feldspar (25 %) and minor opaque oxides (2 %). A typical mineral assemblage is Grt+Crd+Sill+Bt+Kfs+Pl+Qtz (Fig. 2a–d).

3.b. Sillimanite-garnet granite gneiss

Sillimanite-garnet granite gneiss (sample 06H-13) was collected from the Ussuri (Wusuli) River at Hutou (GPS: 46°58′45.7″ N, 133°40′15.2″ E; Fig. 1b). It is composed of an allotriomorphic granular aggregate of plagioclase (15 %, An_{30}), perthitic microcline (30 %) and quartz (40 %), and minor amounts of garnet (5 %), sillimanite (5 %), opaque oxides (2 %), and biotite (3 %), with accessory zircon, titanite and monazite. A typical mineral assemblage is Grt+Sill+Bt+Kfs+Pl+Qtz (Fig. 2e, f). The garnet grains average 1 mm in diameter (Fig. 2e, f) and are preferentially associated with opaque minerals and biotite; the latter is commonly altered (in part to white mica) when it is in contact with garnet. Locally, myrmekite is developed at the boundaries between plagioclase and microcline.

Another sillimanite-garnet granite gneiss (sample 06H-14) was collected from the Ussuri (Wusuli) River at Hutou, about 1 km NE of sample 06H-13 (GPS: 45°59′06.9″ N, 133°40′17.3″ E; Fig. 1b). It is composed of quartz, plagioclase, sillimanite and minor microcline, with aligned biotite flakes and large poikiloblasts of garnet up to 1 cm in diameter. The typical mineral assemblage is Grt+Sill+Bt+Kfs+Pl+Qtz. Areas containing garnet are accompanied by coarse-grained elongated quartz and are generally poorer in biotite.

4. SHRIMP U–Pb analytical methods

The samples of the Hutou complex were processed by crushing, initial heavy liquid and subsequent magnetic separation using a Frantz isodynamic separator. Zircons from the non-magnetic fractions were hand-picked and mounted, along with several pieces of the CZ3 zircon standard, onto adhesive tape, enclosed in epoxy resin and then ground and polished to about half their thickness. The mount was then cleaned and gold-coated and photographed in reflected and transmitted light. Cathodoluminescence (CL) imaging was carried out using a Philips XL30 scanning electron microscope (SEM) at Curtin University of Technology. U–Th–Pb analyses were conducted using a WA Consortium SHRIMP II ion microprobe housed at Curtin University of Technology. Detailed analytical procedures followed those of Nelson (1997) and Williams (1998). Isotopic ratios were monitored by reference to Sri Lankan gem zircon standard (CZ3) with a $^{206}Pb/^{238}U$ ratio of 0.0914 that is equivalent to an age of 564 Ma. Pb/U ratios in the unknown samples were corrected using the ln(Pb/U)/ln(UO/U) relationship as measured on CZ3. All ages have been calculated using the U and Th decay constants recommended by Steiger & Jäger (1997). Reported ages represent $^{206}Pb/^{238}U$ data that have been corrected using the measured ^{204}Pb. The analytical data were reduced, calculated and plotted using the Squid (1.0) and IsoplotEx 2.46 programs (Ludwig, 2001). Individual analyses in the data table and concordia plots are reported at the 1σ level and uncertainties in weighted mean ages are quoted at the 95 % confidence level (2σ), unless otherwise indicated.

5. SHRIMP U–Pb zircon data

5.a. Sillimanite gneiss (sample 06H-12)

Zircons from sillimanite gneiss sample 06H-12 are colourless, transparent and are mostly round to irregularly elongate in shape. They range from about 50 to 100 μm in length, with length to width ratios of 1:1 to 2:1. CL imaging reveals that many grains have a core–rim structure. The rims are generally dark with weak sector or turbulent, irregular zoning (Fig. 3a). The cores show weak oscillatory zoning, with some being small and irregular and appearing bright in CL (Fig. 3a). A total of 19 analyses were made on 15 zircons from sample 06H-12 (Table 1; Fig. 3b). They have overall U and Th contents and Th/U ratios ranging from 114 to 4618 ppm, 6 to 135 ppm and 0.01 to 0.70, respectively. Nine data points are concordant and cluster around 500 Ma (Fig. 3b), defining a weighted mean $^{206}Pb/^{238}U$ age of 490 ± 4 Ma (MSWD = 0.43). These analyses are all from rim domains and have low Th/U ratios of ~ 0.02, indicating that their age records the time of high-grade metamorphism. The other ten spots reveal a lack of grouping and show a spread of $^{206}Pb/^{238}U$ ages down concordia from 934 ± 12 to 440 ± 5 Ma (Table 1). The older dates are recorded from zircon cores that exhibit weak oscillatory zoning (Fig. 3a) and relatively low U and Th contents with high Th/U ratios (0.29–0.46, Table 1), typical of magmatic zircon. This indicates that ages ranging from 900 Ma to 700 Ma are from detrital zircons incorporated in the original sedimentary protolith. In addition, five of the analysed grains give younger $^{206}Pb/^{238}U$ ages of 477 ± 6 to 440 ± 5 Ma (grains H12–4.1, H12–6, H12–15, H12–17 and H12–18). All data were recorded from zircon rims with low Th/U ratios and high U contents. They are mostly discordant and likely record variable amounts of Pb loss, perhaps partially reset by younger granitoid emplacement at *c.* 112 Ma that has been recorded from the area (Wilde, Wu & Zhao, 2010).

https://doi.org/10.1017/S0016756810000063 Published online by Cambridge University Press

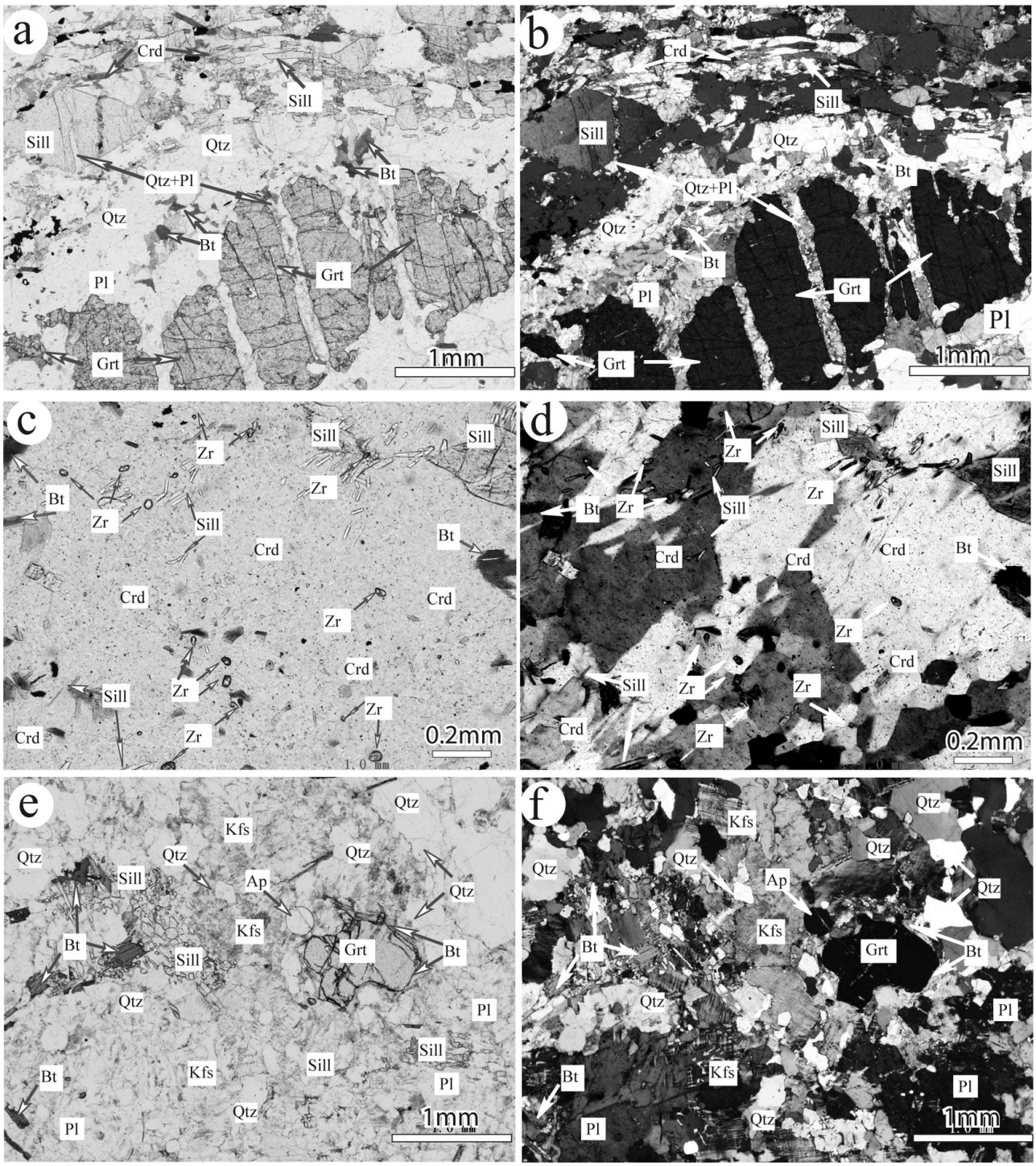

Figure 2. Photomicrographs of analysed samples from the Hutou complex of the Khanka Massif. (a) Typical mineral assemblage of Grt+Crd+Sill+Bt+Kfs+Pl+Qtz in sillimanite gneiss from sample 06H-12 (plane polarized light) and (b) crossed polars. Note: plagioclase+quartz occur in fractures cutting garnet porphyroblasts. (c) Sillimanite, zircon and biotite inclusions in cordierite from sample 06H-12 (plane polarized light) and (d) crossed polars. (e) Typical mineral assemblage of Grt+Sill+Bt+Kfs+Pl+Qtz in sillimanite-garnet granite gneiss sample 06H-13 (plane polarized light) and (f) crossed polars. Note: that biotite rims garnet and apatite is also present. Abbreviations: Grt – garnet; Crd – cordierite; Sill – sillimanite; Bt – biotite; Kfs – K-feldspar; Pl – plagioclase; Qtz – quartz; Zr – zircon and Ap – apatite.

5.b. Sillimanite-garnet granite gneiss

5.b.1. Sample 06H-13

Zircons from sample 06H-13 are colourless, transparent and prismatic, with well-defined pyramidal terminations and a general subhedral shape (Fig. 4a). They range in length from about 80 to 120 μm, with length to width ratios of 2:1 to 4:1. CL imaging reveals that most grains have a core–rim structure. They have thin dark rims that are unzoned or show weak sector zoning, whereas most of the cores have well-defined oscillatory or planar zoning (Fig. 4a). A total of 12

https://doi.org/10.1017/S0016756810000063 Published online by Cambridge University Press

Table 1. SHRIMP Zircon U–Pb data for the Hutou complex in the Khanka Massif

Spot number	U ppm	Th ppm	Th/U	$^{204}Pb/^{206}Pb$	$^{207}Pb^*/^{206}Pb^*$	±%	$^{207}Pb^*/^{235}U$	±%	$^{206}Pb^*/^{238}U$	±%	$^{206}Pb^*/^{238}U$ age (Ma)		$^{207}Pb^*/^{206}Pb^*$ age (Ma)		% Discordance
Sample 06H-12															
H12-1^R	1187	28	0.02	0.000000	0.0570	0.8	0.62	1.5	0.0784	1.2	487	6	492	17	1
H12-2^R	1303	11	0.01	0.000038	0.0566	0.9	0.61	1.5	0.0787	1.2	489	6	476	19	−3
H12-3^R	4618	135	0.03	0.000013	0.0555	2.5	0.62	2.9	0.0809	1.5	502	7	433	56	−14
H12-4^C	368	103	0.29	0.000076	0.0680	1.4	1.14	1.9	0.1216	1.3	740	9	870	28	18
H12-4.1^R	784	6	0.01	0.000008	0.0562	0.9	0.57	1.6	0.0741	1.3	461	6	459	20	0
H12-5^C	199	65	0.34	0.000228	0.0603	4.7	0.83	5.0	0.0993	1.8	610	11	616	101	1
H12-6^R	1035	20	0.02	0.000006	0.0580	0.7	0.56	1.5	0.0707	1.3	440	5	529	16	20
H12-7^R	1176	19	0.02	0.000056	0.0577	1.2	0.62	1.7	0.0781	1.3	485	6	519	25	7
H12-8^R	848	18	0.02	0.000055	0.0578	1.0	0.64	1.6	0.0798	1.3	495	6	522	22	5
H12-9^R	860	7	0.01	0.000013	0.0569	0.9	0.62	1.5	0.0796	1.3	494	6	487	19	−1
H12-10^C	114	77	0.70	0.000221	0.0639	6.0	1.19	6.3	0.1351	1.7	817	13	738	127	−10
H12-11^R	1549	21	0.01	0.000069	0.0564	0.9	0.62	1.5	0.0795	1.3	493	6	467	20	−5
H12-12^C	228	101	0.46	0.000079	0.0752	1.7	1.62	2.2	0.1560	1.4	934	12	1073	35	15
H12-13^M	496	6	0.01	0.000094	0.0577	1.8	0.67	2.2	0.0847	1.3	524	7	519	39	−1
H12-14^R	1436	63	0.05	0.000074	0.0571	0.8	0.62	1.5	0.0783	1.2	486	6	497	18	2
H12-15^R	1173	15	0.01	0.000014	0.0577	0.8	0.58	2.3	0.0726	2.2	452	10	518	17	15
H12-16^R	1322	23	0.02	0.000047	0.0565	0.9	0.62	1.5	0.0796	1.3	494	6	472	19	−4
H12-17^R	1388	16	0.01	0.000013	0.0569	0.7	0.59	1.4	0.0754	1.3	468	6	488	16	4
H12-18^R	1024	13	0.01	0.000083	0.0564	1.0	0.60	1.7	0.0769	1.4	477	6	467	23	−2
Sample 06H-13															
H13-1.1^M	948	291	0.32	0.000009	0.0578	0.7	0.64	2.0	0.0802	1.9	497	9	522	8	5
H13-2.1^R	2969	104	0.04	0.000023	0.0577	0.5	0.64	2.0	0.0808	1.9	501	9	518	5	4
H13-3.1^C	804	611	0.79	0.000008	0.0580	0.8	0.67	2.1	0.0841	1.9	520	10	531	9	2
H13-4.1^M	427	142	0.34	0.000187	0.0549	2.5	0.62	3.2	0.0813	2.0	504	10	409	28	−19
H13-5.1^C	1456	270	0.19	0.000099	0.0579	1.0	0.68	2.1	0.0849	1.9	525	10	527	11	0
H13-6.1^C	1230	217	0.18	0.000013	0.0573	0.8	0.67	2.1	0.0843	1.9	522	10	501	9	−4
H13-7.1^C	1312	1022	0.81	0.000090	0.0574	0.9	0.67	2.1	0.0844	1.9	522	10	506	9	−3
H13-8.1^R	3927	180	0.05	0.000019	0.0576	0.5	0.66	2.0	0.0824	1.9	511	9	516	6	1
H13-9.1^M	1050	217	0.21	0.000024	0.0572	1.5	0.64	2.5	0.0805	1.9	499	9	501	17	0
H13-10.1^R	3030	184	0.06	0.000028	0.0572	0.5	0.66	2.0	0.0831	1.9	515	9	500	6	−3
H13-11.1^R	731	44	0.06	0.000061	0.0575	1.2	0.65	2.3	0.0821	1.9	509	9	510	13	0
H13-12.1^C	253	123	0.50	0.000001	0.0581	1.4	0.66	2.4	0.0821	2.0	509	10	535	15	5
Sample 06H-14															
H14-1.1^C	1234	439	0.37	0.000031	0.0576	1.4	0.66	3.3	0.0830	2.9	514	15	514	31	0
H14-2.1^C	922	250	0.28	0.000006	0.0583	0.7	0.66	2.2	0.0820	2.0	508	10	541	8	6
H14-3.1^C	541	271	0.52	0.000046	0.0580	2.1	0.66	3.4	0.0829	2.6	514	13	530	46	3
H14-4.1^C	846	84	0.10	0.000028	0.0580	0.8	0.66	2.1	0.0829	1.9	514	10	529	9	3
H14-5.1^C	587	136	0.24	0.000104	0.0581	1.6	0.68	2.9	0.0842	2.4	521	12	535	34	3
H14-6.1^C	707	97	0.14	0.000003	0.0579	0.8	0.67	2.1	0.0837	1.9	518	10	528	9	2
H14-7.1^C	850	82	0.10	0.000009	0.0574	0.8	0.66	2.1	0.0834	1.9	516	10	506	8	−2
H14-8.1^C	2508	733	0.30	0.000141	0.0574	0.8	0.64	2.5	0.0809	2.4	502	11	506	17	1
H14-9.1^C	598	268	0.46	0.000013	0.0584	0.9	0.66	2.1	0.0824	1.9	510	10	544	10	7
H14-10.1^C	886	347	0.40	0.000005	0.0576	0.7	0.67	2.1	0.0840	1.9	520	10	516	8	−1
H14-11.1^C	824	136	0.17	0.000010	0.0579	0.8	0.66	2.5	0.0830	2.4	514	12	524	18	2
H14-12.1^C	837	349	0.43	0.000001	0.0581	0.7	0.67	2.1	0.0836	2.0	518	10	532	8	3

Note: ^{C} – analyses from core, ^{R} – analyses from rim and ^{M} – analyses from core–rim mixture.
Errors are 1-sigma and Pb* indicates the radiogenic portions.
Data were ^{204}Pb corrected, using measured values.
% discordance defined as $(((^{207}Pb/^{206}Pb\ age)/(^{206}Pb/^{238}U\ age) - 1) \times 100$.

analyses were made on 10 zircons (Table 1; Fig. 4b). They have overall U and Th contents and Th/U ratios ranging from 253 to 3927 ppm, 44 to 1022 ppm and 0.04 to 0.81, respectively. All analyses are concordant to slightly discordant (Fig. 4b) and, taken together, define a weighted mean $^{206}Pb/^{238}U$ age of 511 ± 6 Ma (MSWD = 1.07). Both the oscillatory zoned cores and dark rims show high contents of U and Th, but can generally be distinguished by the lower Th/U ratios of the latter (Table 1). While there is some overlap with respect to Th/U ratios, in general the metamorphic rims have lower ratios and younger ages. Thus ages clustering at *c.* 510 Ma may be considered as metamorphic recrystallization of oscillatory-zoned igneous zircon formed at between *c.* 520–510 Ma, identical to the features and ages described from deformed and metamorphosed granitoids in the Jiamusi Massif by Wilde, Wu & Zhang (2003). Indeed, reprocessing of the data based on the CL and Th/U ratios allows a distinction to be made between the two groups. Four concordant cores define a weighted mean age of 522 ± 5 Ma (MSWD = 0.38) and four

https://doi.org/10.1017/S0016756810000063 Published online by Cambridge University Press

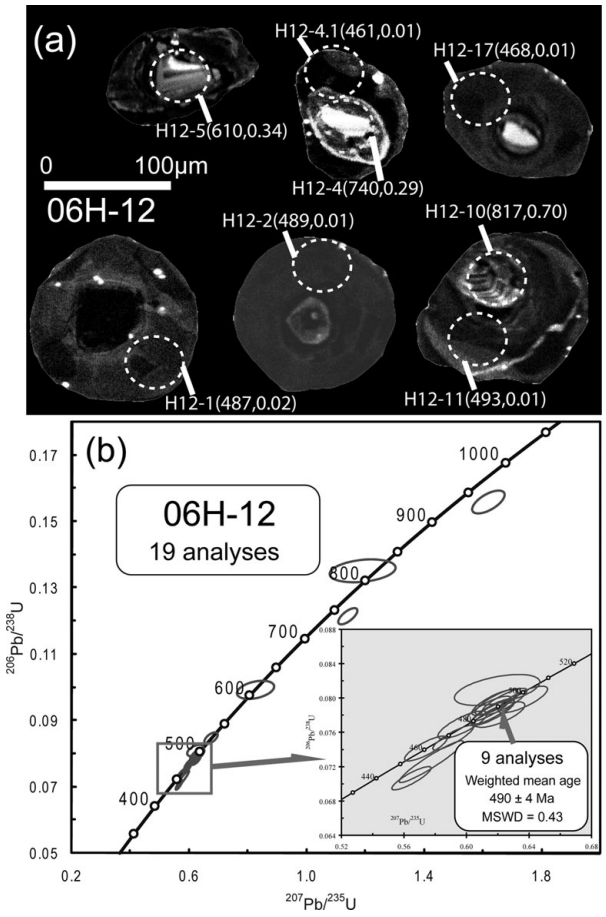

Figure 3. (a) Representative cathodoluminescence (CL) images of zircons from sillimanite paragneiss sample 06H-12; (b) U–Pb concordia diagram of zircon data for sample 06H-12 from the Hutou complex of the Khanka Massif. Note: dashed circles mark sites of SHRIMP analyses. The notation for each spot consists of spot number as in Table 1 and, in brackets, the $^{206}Pb/^{238}U$ age and Th/U ratio.

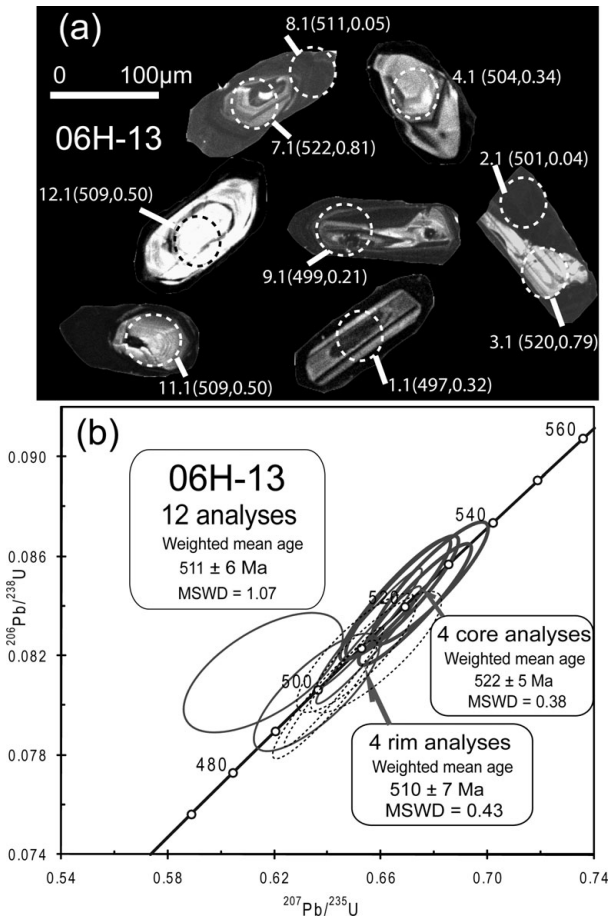

Figure 4. (a) Representative cathodoluminescence (CL) images of zircons from sillimanite-garnet granite gneiss sample 06H-13; (b) U–Pb concordia diagram of zircon data for sample 06H-13 from the Hutou complex of the Khanka Massif. Note: dashed circles mark sites of SHRIMP analyses. The notation for each spot consists of spot number as in Table 1 and, in brackets, the $^{206}Pb/^{238}U$ age and Th/U ratio.

concordant rim analyses define a weighted mean age of 510 ± 7 Ma (MSWD = 0.43), separable within the 2σ errors (Fig. 4b).

5.b.2. Sample 06H-14

Similar to sample 06H-13, zircons from sample 06H-14 are colourless, transparent and prismatic subhedral. They range from about 90 to 120 μm in length, with length to width ratios of 2:1 to 4:1. CL imaging reveals that many grains have a core–rim structure, although the rims are not always continuous and locally appear to grade into the oscillatory zoned core (grain 7 in Fig. 5a). Analytical results for 12 spots (11 zircon cores and one rim (spot 4.1)) are presented in Table 1 and shown on a concordia diagram in Figure 5b. The U and Th contents and Th/U ratios range from 541 to 2508, 82 to 733 and 0.10 to 0.52, respectively. All 12 analyses show a tight, concordant grouping defining a weighted mean $^{206}Pb/^{238}U$ age of 515 ± 8 Ma. No distinction can be made for this sample between the age of the metamorphic rim and the oscillatory zoned cores. Because the rim data are limited to one analysis only (mainly because they were too narrow to analyse), and given the structural evidence of a gradation between core and rim in CL, we interpret the age of 515 ± 8 Ma as recording the crystallization age of the granite protolith. There is thus no real constraint on the timing of high-grade metamorphism affecting this sample, although it is quite likely at *c.* 510–500 Ma, as in nearby sample 06H-13.

6. Discussion

6.a. Protolith age of the sillimanite gneiss

The spread of older zircon ages in sillimanite gneiss sample 06H-12 is best explained by considering the origin of the rock. It would have originally been an aluminous sediment and the zircons may be regarded as detrital grains which were incorporated in the sedimentary precursor during deposition. In favour of this interpretation is the fact that there are several concordant to only weakly discordant zircon grains present with ages of 934 ± 12, 817 ± 13, 740 ± 9 and 610 ± 11 Ma (Table 1; Fig. 3a, b). The morphology

https://doi.org/10.1017/S0016756810000063 Published online by Cambridge University Press

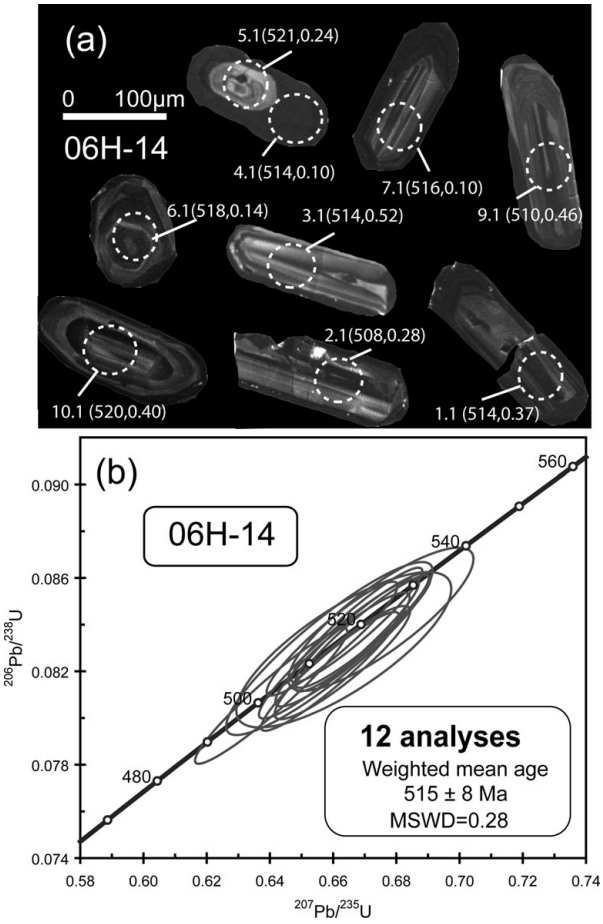

Figure 5. (a) Representative cathodoluminescence (CL) images of zircons from sillimanite-garnet granite gneiss sample 06H-14; (b) U–Pb concordia diagrams of zircon data from sample 06H-14. Note: dashed circles mark sites of SHRIMP analyses. The notation for each spot consists of spot number as in Table 1 and, in brackets, the $^{206}Pb/^{238}U$ age and Th/U ratio.

and internal structure shown by CL imaging reveal that the older zircons are irregular cores with oscillatory zoning (Fig. 3a), suggesting that they were of magmatic origin and were significantly modified during the later high-grade metamorphic event. Although another grain (H12–13) is apparently younger (524 Ma), the low Th/U suggests that the analysis is from a metamorphic rim rather than a core. However, the age is greater than for the other rims and it appears likely that the analysis site inadvertently is a mixture of both core and rim (Table 1). These data are thus considered to limit the time of deposition of the sedimentary rocks (protolith of the sillimanite gneiss) to later than 610 Ma. It seems likely that the main detritus for the sedimentary rocks at Hutou was therefore derived from Neoproterozoic sources.

The only other metasedimentary rock dated from the Khanka Massif is a fine-grained clinopyroxene-bearing gneiss (Wilde, Wu & Zhao, 2010) obtained from Mt Huoshi (Fig. 1b). This is a complex sample that not only records a metamorphic event at 504 ± 8 Ma but also contains younger zircons that cluster at 258 ± 5 Ma, interpreted to be the result of the emplacement of Permian granitoids at depth (Wilde, Wu & Zhao, 2010). It also contains three older detrital igneous zircons with $^{206}Pb/^{238}U$ ages of 942 ± 19, 771 ± 12 and 609 ± 11 Ma, these being essentially similar, within errors, to the data obtained in the present study. In addition, a sillimanite gneiss from Xi Mashan in the adjacent Jiamusi Massif likewise records a *c.* 500 Ma metamorphic event and also contains a suite of detrital zircons whose concordant to slightly discordant $^{206}Pb/^{238}U$ (< 1.0 Ga) and $^{207}Pb/^{206}Pb$ (> 1.0 Ga) ages are grouped at 1.6, 1.4, 1.2, 1.05, 0.6, 0.9 and 0.7 Ga.

6.b. Protolith ages of the sillimanite-garnet granite gneiss

The SHRIMP zircon U–Pb data for the two samples of sillimanite-garnet granite gneiss from the northern and southern parts of the Hutou complex (Fig. 1b) yield ages of 515 ± 8 Ma (Fig. 4b) and 511 ± 6 Ma (Fig. 5b), respectively, which are consistent within analytical errors. Most zircon cores show well-defined oscillatory zoning in CL images (Figs 4a, 5a) and have high Th/U ratios, indicating that the dates may reflect the protolith age of the granite gneiss. Although no metamorphic age could be determined for sample 06H-14 from the northern outcrop, it was possible to discriminate between a protolith age of 522 ± 5 Ma and metamorphic growth/recrystallization of zircon at 510 ± 7 Ma in sample 06H-13 from the more southerly outcrop (Fig. 1).

Two other granitoids have previously been dated from the Hutuo area (Wilde, Wu & Zhao, 2010), both of which contain garnet, but with no record of sillimanite. One sample (FW04-202) is similar to the current sample 06H-13 in showing a mixture of core and rim ages. Here, the older population of igneous zircon records a weighted mean $^{206}Pb/^{238}U$ age of 518 ± 7 Ma, whereas the younger population of metamorphic zircon has a weighted mean $^{206}Pb/^{238}U$ age of 499 ± 10 Ma. Although these ages are slightly younger than the results for sample 06H-13 in this study, they overlap within errors. Unlike our sample 06H-14, which records only the igneous protolith age, sample FW04-207 reported by Wilde, Wu & Zhao (2010) is more extensively recrystallized and only records the metamorphic age of 499 ± 4 Ma. Importantly, similar ages have been reported from deformed granitoids in the Jiamusi Massif (Wilde, Wu & Zhang, 2003). They were likewise interpreted, based on CL studies, as reflecting a high-grade metamorphic overprint of a slightly older igneous population. In summary, the granite gneiss protolith ages of 522–515 Ma are consistent with the ages of 523–515 Ma reported from the Mashan Complex in the Jiamusi Massif (Wilde, Wu & Zhang, 2003).

6.c. Timing of granulite-facies metamorphism

Zircon grains in the sillimanite gneiss (06H-12) mostly have a core–rim structure in CL, and nine analyses of the rims have low Th/U ratios (0.01–0.05) with a

https://doi.org/10.1017/S0016756810000063 Published online by Cambridge University Press

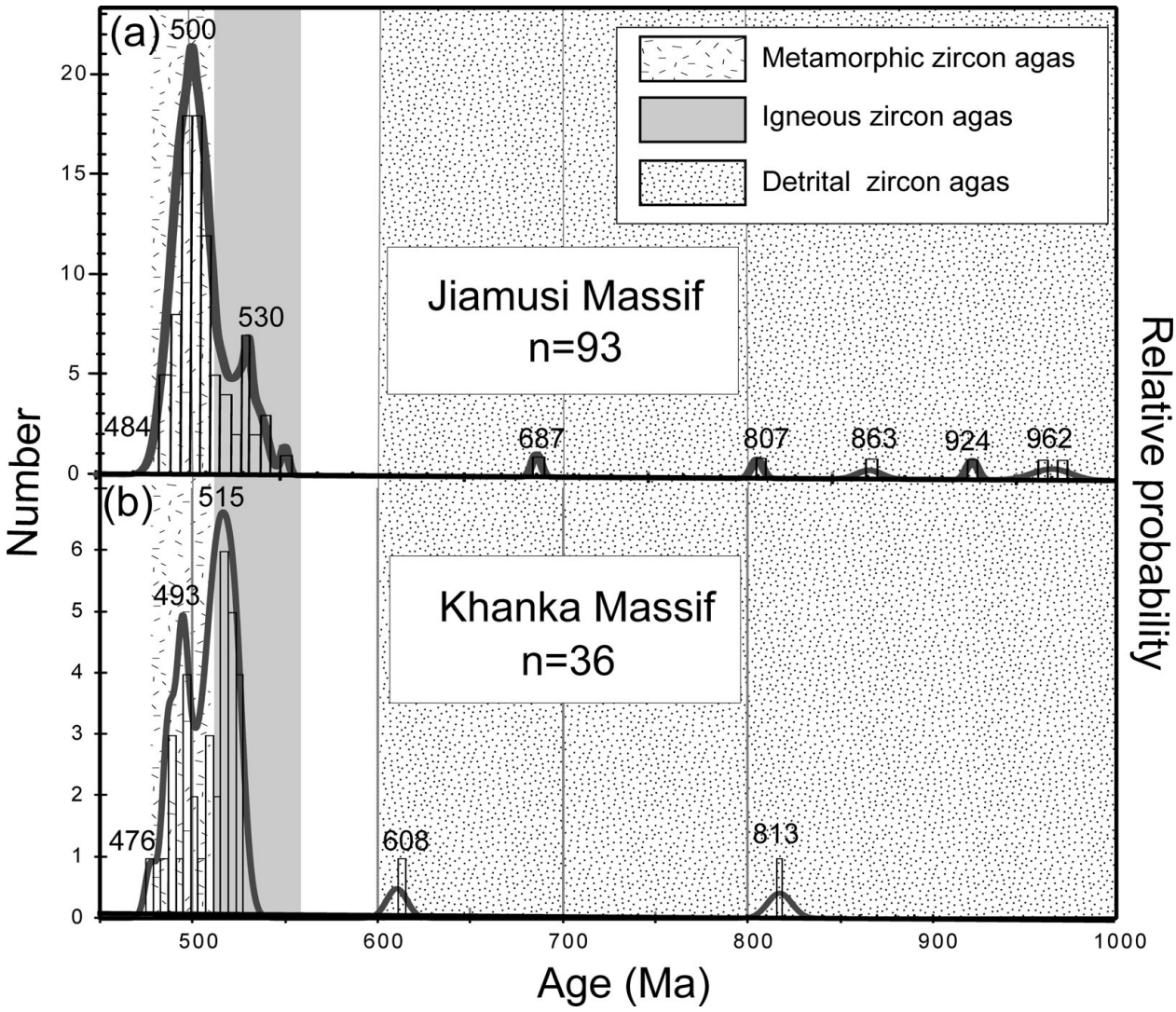

Figure 6. Relative probability plot of samples from (a) the Mashan complex in the Jiamusi Massif compared with zircon ages from (b) the Hutou complex, data from samples 06H-12, 06H-13 and 06H-14 in this study. Data in (a) from Wilde, Dorsett-Bain & Liu, 1997; Wilde, Dorsett-Bain & Lennon, 1999; Wilde, Zhang & Wu, 2000; Wilde, Wu & Zhang, 2003.

weighted mean $^{206}Pb/^{238}U$ age of 490 ± 4 Ma, which records the time of metamorphism in this sample. The sillimanite-garnet granite gneiss samples (06H-13 and 06H-14) also contain zircons that show core–rim structure, but unfortunately many of the rims (especially in 06H-14) were too narrow to analyse. The four most concordant rim ages from sample 06H-13 range between 515 ± 9 and 501 ± 9 Ma with a weighted mean of 510 ± 7 Ma, taken to record the time of metamorphism. For sample 06H-14, the rims are much less common and only one was analysed (06H-14-1.1); it recorded an age of 514 ± 15 Ma (Table 1; Fig. 5a), indistinguishable from the oscillatory zoned cores. Taken together with the metamorphic age of 490 ± 4 Ma from paragneiss sample 06H-12, it indicates that the high-grade metamorphism occurred at *c.* 500 Ma.

The time of metamorphism in the Hutuo area from the data of Wilde, Wu & Zhao (2010) was 504 ± 8 Ma for a fine-grained paragneiss, but ranged from 491 ± 4 to 499 ± 10 Ma for their two garnet-bearing granitoids. These ages are similar to our new data, within error. The timing of high-grade metamorphism at *c.* 500 Ma has been reported from widely distributed samples of both ortho- and paragneiss in the Mashan Complex of the Jiamusi Massif (Wilde, Dorsett-Bain & Liu, 1997; Wilde, Dorsett-Bain & Lennon, 1999; Wilde, Zhang & Wu, 2000); events were thus coeval in the Khanka and Jiamusi massifs.

6.d. Tectonic affinity of the Khanka Massif

The new SHRIMP data from the Hutou complex of the Khanka Massif essentially show three age populations (Fig. 6b): 480–500 Ma with a peak at *c.* 493 Ma, interpreted as recording the time of metamorphism; 510–525 Ma with the peak age of 515 Ma, indicating the protolith age of the granitoids; and 610–817 (934 obtained from a zircon 15 % discordant) Ma, considered to be the age of detrital magmatic zircon, attesting to the existence of a significant volume of Neoproterozoic rocks in the source area of the

https://doi.org/10.1017/S0016756810000063 Published online by Cambridge University Press

original sedimentary rocks. Rocks of the Mashan Complex in the adjacent Jiamusi Massif show very similar age populations (Fig. 6a): 484–510 Ma with a peak age at *c.* 500 Ma, recording the time of high-grade metamorphism; 510–550 Ma with a peak at 530 Ma, recording the protolith ages of the deformed granitoid rocks; and 687–962 Ma, indicating the age of Neoproterozoic detrital zircons derived from the source area of the clastic metasedimentary rocks of the Mashan Complex. These results substantiate the view that the Khanka and Jiamusi massifs underwent an identical tectonic evolution and should therefore be regarded as forming part of a contiguous block from Late Neoproterozoic time (Wilde, Wu & Zhao, 2010).

In terms of the overall tectonic setting, some models have suggested that the Khanka Massif belongs to the South China Craton and, together with the Heilongjiang Complex, forms an extension of the east–west-trending Dabie-Sulu UHP belt (Zhang, 1997, 2004; Zhang, Cai & Zhu, 2006). Oh (2006) suggested that the Khanka Massif was a continuation of Dabie-Sulu belt along the northern boundary of the North China Craton, but that the Bureya Massif was not part of either the North or South China Craton (Oh & Kusky, 2007).

The basement rocks of the North and South China Cratons record very different thermo-magmatic histories before they finally came together in the Early Mesozoic (e.g. Zheng *et al.* 2003, 2005; Grimmer *et al.* 2003; Hacker, McClelland & Liou, 2006; Ratschbacher *et al.* 2006; Zhou *et al.* 2008*a*) and it is relatively easy to discriminate between them. In particular, Precambrian basement rocks of the North China Craton are dominated by Neoarchaean granitoids and orthogneisses (mostly tonalite–trondhjemite–granodiorite) and Palaeoproterozoic metasedimentary sequences (e.g. Zhao *et al.* 2000, 2002, 2005; Wilde & Zhao, 2005; Zhai, Guo & Liu, 2005; Wan *et al.* 2006; Zhou *et al.* 2008*b*). Protolith ages for the orthogneisses and the granitoids are mostly in the range of 2.9–2.5 Ga (Zhao *et al.* 2000, 2002, 2005; Zhai, Guo & Liu, 2005; Wilde & Zhao, 2005; Zhou *et al.* 2008*b*) and underwent 1.9–1.8 Ga regional amphibolite- to granulite-facies metamorphism (Zhao *et al.* 2000, 2005; Santosh, Sajeev & Li, 2006; Zhou *et al.* 2008*b*). In contrast, the South China Craton is characterized by young basement of Meso- to Neoproterozoic age that was subjected to major thermal events during Neoproterozoic times (1.1–1.0 Ga and 850–700 Ma) (Li *et al.* 2002, 2003; Zheng *et al.* 2003, 2005; Zhou *et al.* 2008*c*), Although granulite-facies rocks are present in the Jiaobei area (Jiangshan Group) of the Dabie-Sulu belt (Zhou *et al.* 2008*b*,*d*), the metamorphic ages are 1.86–1.80 Ga (zircon U–Pb age, Zhou *et al.* 2008*d*), quite different from the metamorphic age of *c.* 500 Ma for the Hutou complex. Precambrian basement in the South China Craton is further characterized by the widespread occurrence of 820–740 Ma bimodal igneous rocks formed in rift settings (Li *et al.* 2002, 2003; Zheng *et al.* 2003, 2005; Zhou *et al.* 2008*c*). Granulite-facies rocks are also present in the Huangtuling area of the northern Dabie belt (Wu *et al.* 2002), where the metamorphic age is 2052 ± 1 Ma (SHRIMP zircon U–Pb age, Wu *et al.* 2002), quite different from the metamorphic age of *c.* 500 Ma for the Hutou complex. There is no evidence for a *c.* 500 Ma granulite-facies event in either the North or South China Craton and thus the Khanka Massif cannot be related to these cratons.

One fact that needs to be considered is the presence of mixed Permian faunas in the Yanji area of the Khanka Massif, characterized by an admixture of both palaeo-tropical Cathaysian taxa and cool-temperate elements (e.g. Shao & Tang, 1995; Shao, Tang & Zhan, 1995; Ren *et al.* 1999). While this has been used as evidence indicating that the Khanka Massif has a South China Craton affinity (e.g. Shao & Tang, 1995; Shao, Tang & Zhan, 1995; Zhang, 1997, 2004; Zhang, Cai & Zhu, 2006; Ren *et al.* 1999), Shi (2006), Shi & Zhan (1996) and Li (2006) have pointed out that such mixed Permian faunas are not only found in the Yanji area, but also in other parts of the Central Asian Orogenic Belt. In particular, since the Khanka Massif is located at the easternmost part of the CAOB at its boundary with the Palaeo-Pacific Ocean, palaeo-tropical Cathaysian taxa might have crossed the Palaeo-Pacific Ocean during Permian times (Shi, 2006).

Other suggestions are that the Jiamusi/Khanka Massif was a crustal fragment derived from a peri-Gondwana position that drifted northward and collided with the CAOB collage in the Late Permian (Wilde, Wu & Zhang, 2003), that it was possibly related to the margin of the Siberia Craton (Wilde, Dorsett-Bain & Liu, 1997), or that it was an exotic block of unknown affinity that collided with the CAOB in the Early Jurassic as a result of Pacific Plate subduction (Wu *et al.* 2007).

With respect to Siberia, Salnikova *et al.* (1998, 2001) and Khain *et al.* (2003) recognize a high-grade Palaeozoic metamorphic terrain that extends for more than 1000 km along the southern margin of the Siberia Craton. Salnikova *et al.* (1998) reported single-grain zircon $^{206}Pb/^{238}U$ ages of 488 ± 1 Ma for pyroxene-bearing trondhjemite emplaced during granulite-facies metamorphism of the Sludyanskiy Complex in the southwestern Baikal region, at the southern margin of the Siberia Craton (Fig. 1a). In addition, single metamorphic zircons from a two-pyroxene trondhjemite define peak metamorphism in the Sludyanskiy Complex at 478 ± 2 Ma ($^{206}Pb/^{238}U$ age), whereas a post-metamorphic pyroxene-bearing quartz syenite, with a zircon multi-grain $^{206}Pb/^{238}U$ age of 471 ± 2 Ma, indicates that the metamorphic episode was short-lived and only lasted for *c.* 20 Ma. However, there are currently few precise age data for the areas between the Jiamusi/Khanka Massif and the Siberia Craton, so at present it is impossible to know the significance of this potential link.

https://doi.org/10.1017/S0016756810000063 Published online by Cambridge University Press

7. Conclusions

(1) The Khanka Massif is located adjacent to the Late Jurassic–Early Cretaceous circum-Pacific accretion complexes in NE China and Far East Russia, with the Chinese part only well exposed in the Hutou area. The rocks here constitute a khondalitic sequence of graphite-, sillimanite- and cordierite-bearing gneisses, carbonates and felsic paragneisses, intruded by deformed granitoids, some of which are sillimanite- and garnet-bearing. SHRIMP zircon U–Pb dating indicates that these rocks underwent granulite-facies metamorphism at *c.* 500 Ma.

(2) SHRIMP zircon U–Pb dating of a sillimanite gneiss indicates several detrital zircon grains whose ages extend back to 934 Ma. These data indicate that the source region providing detritus for sedimentation in the Khanka Massif contained significant Neoproterozoic components.

(3) Two samples of sillimanite-garnet granite gneiss from the Hutou complex contain zircon cores that yield magmatic weighted mean $^{206}Pb/^{238}U$ ages of 522 ± 5 Ma and 515 ± 8 Ma, whereas their metamorphic rims record $^{206}Pb/^{238}U$ ages of 510–500 Ma. These data indicate that the Hutou complex records Early Palaeozoic magmatic and metamorphic events equated with the Late Pan-African global event.

(4) These data, when taken together with other recent data obtained from the Khanka Massif, establish that the nature and timing of Early Palaeozoic events are identical to those in the adjacent Jiamusi Massif. The two massifs should thus be considered as constituting a single crustal entity.

(5) The tectonic affinity of the Khanka/Jiamusi Massif remains unresolved. While it is possible to rule out a connection with the South China Craton and North China Craton, it is not possible to say if it formed an exotic block related to the dispersal of Gondwana and/or the onset of Pacific Plate subduction from the east, or whether it is related in some way to similar-aged rocks developed along the southern margin of the Siberia Craton; further work is required to resolve this issue.

Acknowledgements. This study was funded by grants from the Natural Science Foundation of China (40672148, 40739905 and 40872121), Ph.D. Programs Foundation of Ministry of Education of China (20090061110048) and the Ministry of Science and Technology of the P.R. China (2009CB825008). The final version of the paper has benefited from the perceptive comments of David Pyle (editor), and reviewers Ian S. Williams and Chang Whan Oh. This is The Institute for Geosciences Research (TIGeR) publication No. 205.

References

CAO, X., DANG, Z. X., ZHANG, X. Z., JIANG, J. S. & WANG, H. D. 1992. *Jiamusi Composite Terranes*. Jilin Publishing House of Science and Technology, Changchun 19, 224 pp. (in Chinese, with English and Russian abstracts).

CHENG, R. Y., WU, F. Y., GE, W. C., SUN, D. Y., LIU, X. M. & YANG, J. H. 2006. Emplacement age of the Raohe Complex in eastern Heilongjiang Province and the tectonic evolution of the eastern part of Northeastern China. *Acta Petrologica Sinica* **22**, 353–76.

GRIMMER, C., RATSCHBACHER, L., MCWILLIAMS, M., FRANZ, L., GAITZSCH, I., TICHOMIROWA, M., HACKER, B. R. & ZHANG, Y. 2003. When did the ultra high pressure rocks reach the surface? A $^{207}Pb/^{206}Pb$ zircon, $^{40}Ar/^{39}Ar$ white mica, Si-in-white mica, single-grain provenance study of Dabie Shan synorogenic foreland sediments. *Chemical Geology* **197**, 87–110.

HACKER, B. R., MCCLELLAND, W. C. & LIOU, J. G. 2006. *Ultrahigh-pressure metamorphism: Deep continental subduction.* Geological Society of America, Special Paper no. 403, 206 pp.

HBGMR (HEILONGJIANG BUREAU OF GEOLOGY AND MINERAL RESOURCES). 1993. *Regional Geology of Heilongjiang Province*. Geological Publishing House, 734 pp. (in Chinese with English abstract).

ISHIWATARI, A. & TSUJIMORI, T. 2001. Late Paleozoic High-pressure Metamorphic Belts in Japan and Sikhote-Alin: Possible Oceanic Extension of the Chinese Dabie-Su-Lu Suture Detouring Korea. *Gondwana Research* **4**, 636–8.

ISHIWATARI, A. & TSUJIMORI, T. 2003. Paleozoic ophiolites and blueschists in Japan and Russian Primorye in the tectonic framework of East Asia: A synthesis. *The Island Arc* **12**, 190–206.

JAHN, B. M. 2004. The Central Asian Orogenic Belt and growth of the continental crust in the Phanerozoic. In *Aspects of the Tectonic Evolution of China* (eds J. Malpas, C. J. N. Fletcher, J. R. Ali & J. C. Aitchison), pp. 73–100. Geological Society of London, Special Publication no. 226.

JAHN, B. M., WU, F. Y. & CHEN, B. 2000. Massive granitoid generation in central Asia: Nd isotopic evidence and implication for continental growth in the Phanerozoic. *Episodes* **23**, 82–92.

JIA, D. C., HU, R. Z., LU, Y. & QIU, X. L. 2004. Collision belt between the Khanka block and the North China block in the Yanbian region, northeast China. *Journal of Asian Earth Sciences* **23**, 211–19.

JIANG, J. 1992. Peak regional metamorphism of the khondalite series of Mashan Group and its evolution. *Acta Petrologica et Mineralogica* **11**, 97–108 (in Chinese with English abstract).

KHAIN, E. V., BIBIKOVA, E. V., SALNIKOVA, E. B., KRÖNER, A., GIBSHER, A. S., DIDENKO, A. N., DEGTYAREV, K. E. & FEDOTOVA, A. A. 2003. The Palaeo-Asian Ocean in the Neoproterozoic and early Palaeozoic: new geochronologic data and palaeotectonic reconstructions. *Precambrian Research* **122**, 329–58.

KOJIMA, S. 1989. Mesozoic terrane accretion in northeast China, Sikhote-Alin and Japan regions. *Palaeogeography, Palaeoclimatology, Palaeoecology* **69**, 213–32.

LENNON, R. G., WILDE, S. A. & YANG, T. 1997. The Mashan Group: a 500 Ma granulite facies terrain within the Jiamusi Massif, Heilongjiang Province, North-eastern China. In *Proterozoic Geology of Madagascar* (eds R. Cox & L. D. Ashwal), pp. 45–6. Proceedings of UNESCO-IUGS-IGCP 348/368 International Field Workshop, Antananarivo, Madagascar, 1997. Gondwana Research Group, Publication no. 5.

LI, J. Y. 2006. Permian geodynamic setting of Northeast China and adjacent regions: Closure of the Paleo-Asian Ocean and subduction of the Paleo-Pacific Plate. *Journal of Asian Earth Sciences* **26**, 207–24.

LI, J. Y., NIU, B. G., SONG, B., XU, W. X., ZHANG, Y. H. & ZHAO, Z. R. 1999. Crustal Formation and Evolution of Northern Changbai Mountains, Northeast China. Geological Publishing House, Beijing, pp. 32–50 (in Chinese with English abstract).

LI, Z. X., LI, X. H., KINNY, P. D., WANG, J., ZHANG, S. & ZHOU, H. 2003. Geochronology of Neoproterozoic syn-rift magmatism in the Yangtze Craton, South China and correlations with other continents: evidence for a mantle superplume that broke up Rodinia. *Precambrian Research* **122**, 85–109.

LI, Z. X., LI, X. H., ZHOU, H. & KINNY, P. D. 2002. Grenvillian continental collision in south China: new SHRIMP U–Pb zircon results and implications for the configuration of Rodinia. *Geology* **30**, 163–6.

LUDWIG, K. R. 2001. *Users Manual for Isoplot/Ex (ver. 2.49): A Geochronological Toolkit for Microsoft Excel*. Berkeley Geochronology Center, Special Publication No. 1a, 55 pp.

NATAL'IN, B. A. 1991. Mesozoic accretion and collision tectonics of southern USSR Far East. *Pacific Geology* **10**, 3–23.

NATAL'IN, B. A. 1993. History and modes of Mesozoic accretion in southeastern Russia. *The Island Arc* **2**, 15–34.

NATAL'IN, B. A. & BORUKAYEV, C. B. 1991. Mesozoic sutures in the southern Far East of USSR. *Geotectonics* **25**, 64–74.

NELSON, D. R. 1997. Compilation of SHRIMP U–Pb zircon geochronology data, 1996, Geological Survey of Western Australia. 1997/2, 189 pp.

OH, C. W. 2006. A new concept on tectonic correlation between Korea, China and Japan: Histories from the late Proterozoic to Cretaceous. *Gondwana Research* **9**, 47–61.

OH, C. W., KIM, S. W. & WILLIAMS, I. S. 2006. Spinel granulite in Odesan area, South Korea: Tectonic implications for the collision between the North and South China blocks. *Lithos* **92**, 557–75.

OH, C. W & KUSKY, T. 2007. The Late Permian to Triassic Hongseong-Odesan Collision Belt in South Korea, and Its Tectonic Correlation with China and Japan. *International Geology Review* **49**, 636–57.

RATSCHBACHER, L., FRANZ, L., ENKELMANN, E., JONCKHEERE, R., PORSCHKE, A., HACKER, B. R., DONG, S. & ZHANG, Y. 2006. The Sino-Korean-Yangtze suture, the Huwan detachment, and the Paleozoic–Tertiary exhumation of (ultra) high-pressure rocks along the Tongbai-Xinxian-Dabie Mountains. In *Ultrahigh-pressure metamorphism: Deep continental subduction* (eds B. R. Hacker, W. C. McClelland & J. G. Liou), pp. 45–77. The Geological Society of America, Special Paper no. 403.

REN, J. S., WANG, Z. X., CHEN, B. W., JIANG, C. F., NIU, B. G., LI, J. Y., XIE, G. L., HE, Z. G. & LIU, Z. G. 1999. *The tectonics of China from a global view. A guide to the tectonic map of China and adjacent regions*. Beijing: Geological Publishing House, pp. 4–32.

SALNIKOVA, E. B., KOZAKOV, I. K., KOTOV, A. B., KRÖNER, A., TODT, W., BIBIKOVA, E. V., NUTMAN, A., YAKOVLEVA, S. Z. & KOVACH, V. P. 2001. Age of Palaeozoic granites and metamorphism in the Tuvino-Mongolian Massif of the Central Asian Mobile Belt: loss of a Precambrian microcontinent. *Precambrian Research* **110**, 143–64.

SALNIKOVA, E. B., SERGEEV, S. A., KOTOV, A. B., YAKOVLEVA, S. Z., REZNITSKII, L. Z. & VASIL'EV, E. P. 1998. U–Pb zircon dating of granulite metamorphism in the Slyudyanskiy complex, Eastern Siberia. *Gondwana Research* **1**, 195–205.

SANTOSH, M., SAJEEV, K. & LI, J. H. 2006. Extreme crustal metamorphism during Columbia supercontinent assembly: evidence from North China craton, *Gondwana Research* **10**, 256–66.

ŞENGÖR, A. M. C. & NATAL'IN, B. A. 1996. Paleotectonics of Asia: Fragments of a synthesis. In *The Tectonic Evolution of Asia* (eds A. Yin & T. M. Harrison), pp. 486–640. Cambridge University Press.

ŞENGÖR, A. M. C., NATAL'IN, B. A. & BURTMAN, V. S. 1993. Evolution of the Altaid tectonic collage and Palaeozoic crustal growth in Eurasia. *Nature* **364**, 299–307.

SHAO, J. A. & TANG, K. D. 1995. *Terranes in Northeast China and Evolution of Northeast Asia Continental Margin*. Beijing: Seismology Publishing House, 185 pp. (in Chinese).

SHAO, J. A., TANG, K. D. & ZHAN, L. P. 1995. Reconstruction of an ancient continental margin and its implication: new progress on the study of geology of Yanbian region, northeast China. *Science in China (Series B)* **25**, 548–55.

SHI, G. R. 2006. Marine Permian in East and NE Asia: an overview of biostratigraphy, palaeobiogeography and palaeogeographical implications. *Journal of Asian Earth Sciences* **26**, 175–206.

SHI, G. R. & ZHAN, L. P. 1996. A mixed mid-Permian marine fauna from the Yanji area, northeastern China: a paleobiogeographical reinterpretation, *The Island Arc* **5**, 385–95.

STEIGER, R. H. & JÄGER, E. 1997. Subcommission on geochronology: convention on the use of decay constants in geo- and cosmochronology. *Earth and Planetary Science Letters* **36**, 359–62.

TANG, K. D. 1990. Tectonic development of Paleozoic foldbelts at the northern margin of the Sino–Korean craton. *Tectonics* **9**, 249–60.

TANG, K. D., WANG, Y., HE, G. Q. & SHAO, J. A. 1995. Continental-margin structure of Northeast China and its adjacent areas. *Acta Geologica Sinica* **69**, 16–30.

WAN, Y. S., SONG, B., LIU, D. Y., WILDE, S. A., WU, J. S., SHI, Y. R., YIN, X. Y. & ZHOU, H. Y. 2006. SHRIMP U–Pb zircon geochronology of Palaeoproterozoic metasedimentary rocks in the North China Craton: Evidence for a major Late Palaeoproterozoic tectonothermal event. *Precambrian Research* **149**, 249–71.

WANG, L. W., WANG, Y., YANG, J., WU, G. Q., LI, G. Y. & SHENG, L. 2007. Pre-Mesozoic basement provenance tracing of the Songliao Basin by means of detrital zircon SHRIMP chronology. *Earth Science Frontiers* **14**, 151–8.

WILDE, S. A., DORSETT-BAIN, H. L. & LENNON, R. G. 1999. Geological setting and controls on the development of graphite, sillimanite and phosphate mineralisation within the Jiamusi Massif: an exotic fragment of Gondwanaland located in North-Eastern China? *Gondwana Research* **2**, 21–46.

WILDE, S. A., DORSETT-BAIN, H. L. & LIU, J. L. 1997. The identification of a Late Pan-African granulite facies event in Northeastern China: SHRIMP U–Pb zircon dating of the Mashan Group at Liu Mao, Heilongjiang Province, China, pp. 59–74. *Proceedings of the 30th IGC: 17 Precambrian Geology and Metamorphic Petrology*. Amsterdam: VSP International Science Publishers.

WILDE, S. A., WU, F. Y. & ZHANG, X. Z. 2003. Late Pan-African magmatism in Northeastern China: SHRIMP U–Pb zircon evidence for igneous ages from the Mashan Complex. *Precambrian Research* **122**, 311–27.

WILDE, S. A., WU, F. Y. & ZHAO, G. C. 2010. The Khanka Block, NE China, and its significance to the evolution of the Central Asian Orogenic Belt and continental accretion. In *The Evolved Continents: Understanding the Processes of Continental Growth* (eds T. M. Kusky, M. G. Zhai & W. J. Xiao). Geological Society of London, Special Publication, in press.

WILDE, S. A., ZHANG, X. Z. & WU, F. Y. 2000. Extension of a newly-identified 500 Ma metamorphic terrain in Northeast China: Further U–Pb SHRIMP dating of the Mashan Complex, Heilongjiang Province, China. *Tectonophysics* **328**, 115–30.

WILDE, S. A. & ZHAO, G. C. 2005. Archean to Paleoproterozoic evolution of the North China Craton. *Journal of Asian Earth Sciences* **24**, 519–22.

WILLIAMS, I. S. 1998. U–Th–Pb geochronology by ion microprobe. In *Applications of Microanalytical Techniques to Understanding Mineralizing Processes* (eds M. A. McKibben, W. C. Shanks III & W. I. Ridley), pp. 1–35. *Reviews in Economic Geology* **7**.

WU, F. Y., JAHN, B. M., WILDE, S. A., LO, C. H., YUI, T. F., LIN, Q., GE, W. C. & SUN, D. Y. 2003. Highly fractionated I-type granites in NE China (I): Geochronology and petrogenesis. *Lithos* **66**, 241–73.

WU, F. Y., JAHN, B. M., WILDE, S. A. & SUN, D. Y. 2000. Phanerozoic continental crustal growth: Sr–Nd isotopic evidence from the granites in northeastern China. *Tectonophysics* **328**, 87–113.

WU, F. Y., SUN, D. Y., LI, H. M. & WANG, X. L. 2001. The nature of basement beneath the Songliao Basin in NE China: Geochemical and isotopic constraints. *Physics and Chemistry of the Earth (Part A)* **26**, 793–803.

WU, F. Y., YANG, J. H., LO, C. H., WILDE, S. A., SUN, D. Y. & JAHN, B. M. 2007. Jiamusi Massif in China: a Jurassic accretionary terrane in the western Pacific. *The Island Arc* **16**, 156–72.

WU, Y. B., CHEN, D. G., XIA, Q. K., DELOULE, E. & CHENG, H. 2002. SIMS U–Pb dating of zircons in granulite of Huangtuling from Northern Dabieshan, *Acta Petrologica Sinica* **18**, 378–82.

ZHAI, M. G., GUO, J. H. & LIU, W. J. 2005. Neoarchean to Paleoproterozoic continental evolution and tectonic history of the North China Craton: a review. *Journal of Asian Earth Sciences* **24**, 547–61.

ZHANG, K. J. 1997. North and South China collision along the eastern and southern North China margins. *Tectonophysics* **270**, 145–56.

ZHANG, K. J. 2004. Granulite xenoliths from Cenozoic basalts in SE China provide geochemical fingerprints to distinguish lower crust terranes from the North and South China tectonic blocks: comment. *Lithos* **73**, 127–34.

ZHANG, K. J., CAI, J. X. & ZHU, J. X. 2006. North China and South China collision: Insights from analogue modeling. *Journal of Geodynamics* **42**, 38–51.

ZHAO, C., PENG, Y. & DANG, Z. 1995. *The formation and evolution of crust in Eastern Jilin and Heilongjiang Provinces*. Geotectonic Map of Eastern Jilin and Heilongjiang Provinces. 1:1,500,000 scale map and explanatory notes. Shenyang Institute of Geology and Mineral Resources and Heilongjiang Institute of Geology and Mineral Resources.

ZHAO, G. C., CAWOOD, P. A., WILDE, S. A. & SUN, M. 2002. Review of global 2.1–1.8 Ga orogens: implications for a pre-Rodinia supercontinent. *Earth Science Reviews* **59**, 125–62.

ZHAO, G. C., CAWOOD, P. A., WILDE, S. A., SUN, M. & LU, L. Z. 2000. Metamorphism of basement rocks in the Central Zone of the North China Craton: implications for Paleoproterozoic tectonic evolution. *Precambrian Research* **103**, 55–88.

ZHAO, G. C., SUN, M., WILDE, S. A. & LI, S. Z. 2005. Late Archean to Paleoproterozoic evolution of the North China Craton: key issues revisited. *Precambrian Research* **136**, 177–202.

ZHENG, Y. F., FU, B., GONG, B. & LI, L. 2003. Stable isotope geochemistry of ultrahigh pressure metamorphic rocks from the Dabie-Sulu orogen in China: Implications for geodynamics and fluid regime. *Earth Science Reviews* **62**, 105–61.

ZHENG, Y. F., ZHOU, J. B., WU, Y. B. & XIE, Z. 2005. Low-grade metamorphic rocks in the Dabie-Sulu orogenic belt: a passive-margin accretionary wedge deformed during continent subduction. *International Geology Review* **47**, 851–71.

ZHOU, J. B., WILDE, S. A., ZHANG, X. Z., ZHAO, G. C., ZHENG, C. Q., WANG, Y. J. & ZHANG, X. H. 2009. The onset of Pacific margin accretion in NE China: evidence from the Heilongjiang high-pressure metamorphic belt. *Tectonophysics* **478**, 230–46.

ZHOU, J. B., WILDE, S. A., ZHAO, G. C., ZHENG, C. Q., JIN, W., ZHANG, X. Z. & CHENG, H. 2008*a*. Detrital zircon U–Pb dating of low-grade metamorphic rocks in the Sulu UHP belt: evidence for overthrusting of the North China Craton onto the South China Craton during continental subduction. *Journal of the Geological Society, London* **165**, 423–33.

ZHOU, J. B., WILDE, S. A., ZHAO, G. C., ZHENG, C. Q., JIN, W., ZHANG, X. Z. & CHENG, H. 2008*b*. SHRIMP U–Pb zircon dating of the Neoproterozoic Penglai Group and Archean gneisses from the Jiaobei Terrane, North China Craton, and their tectonic implications. *Precambrian Research* **160**, 323–40.

ZHOU, J. B., WILDE, S. A., ZHAO, G. C., ZHENG, C. Q., JIN, W., ZHANG, X. Z. & CHENG, H. 2008*c*. SHRIMP U–Pb zircon dating of the Wulian Complex: defining the boundary between the North and South China Cratons in the Sulu Orogenic Belt, China. *Precambrian Research* **162**, 559–76.

ZHOU, X. W., ZHAO, G. C., WEI, C. J., GENG, Y. S. & SUN, M. 2008*d* . EPMA, U–Th–Pb monazite and SHRIMP U–Pb zircon geochronology of high-pressure pelitic granulites in the Jiaobei Massif of the North China Craton. *American Journal of Science* **308**, 328–50.

ZYABREV, S. & MATSUOKA, A. 1999. Late Jurassic (Tithonian) radiolarians from a clastic unit of the Khabarovsk complex (Russian Far East): significance for subduction accretion timing and terrane correlation. *The Island Arc* **8**, 30–7.